Available online at www.sciencedirect.com
SCIENCE DIRECT®
Tetrahedron: Asymmetry
Tetrahedron: *Asymmetry* 16 (2005) 2031–2038

Interpenetrating chiral 2D grid nets: hetero- versus homochiral 3D polycatenation in the crystal self-assembly of (*RS*)- and (*R*)-1,1′-binaphthalene-2,2′,6,6′-tetracarboxylic acids

Petr Holý,[a,*] Martin Kováč,[a] Miloš Tichý,[a] Jiří Závada,[a] Miloš Buděšínský[a] and Ivana Císařová[b]

[a]*Institute of Organic Chemistry and Biochemistry, Academy of Sciences of the Czech Republic, Flemingovo nám. 2, 166 10 Prague 6, Czech Republic*
[b]*Department of Inorganic Chemistry, Faculty of Natural Sciences, Charles University, Hlavova 2030, 128 40 Prague 2, Czech Republic*

Received 8 April 2005; accepted 21 April 2005

Abstract—Crystallographic analysis of the title binaphthyl tetracid **2** revealed unique propensity to polycatenation upon crystallization of both the enantiomerically homogeneous as well as the racemic form of the axially chiral tecton. Stereochemical aspects of the polycatenation have been analyzed in three conceptual steps, (i) formation of infinite 2D grids set up from hydrogen-bonded tecton cyclotetramers, (ii) stacking of the 2D grids, and (iii) interpenetration of the resulting stacks. In the crystal self-assembly of the enantiomerically uniform tecton, all three steps are homochiral. Conversely, in the crystal of the racemic tecton the homochiral self-assembling algorithm operates only in the steps (i) and (ii), giving rise to separate, antipodal, stacks of homochiral 2D layers. In the final step (iii), the antipodal stacks mutually interpenetrate, yielding racemic 3D polycatenated architecture within a single crystal.

1. Introduction

Catenanes consist of independent rings that are interlocked. Over the past two decades, several ingenious approaches have been proposed for their template-driven synthesis.[1] At the same time, highly ordered polycatenanes have been discovered by X-ray crystallography to arise spontaneously as a result of mutual interpenetration of two or more independent supramolecular nets in the crystal lattice.[2] We are interested in the self-assembly of chiral porous structures.[3] Recently, we have investigated crystal self-assembly of biphenyl tecton **1** and some of its congeners, and demonstrated[3e] the broad propensity of this family of tectons to the formation of infinite 2D grid layers set up from hydrogen-bonded 'chiral square' cyclotetramers. Herein we have prepared binaphthyl tecton **2**, which may be viewed upon as the expanded homologue of the parent biphenyl tecton **1**.

Formation of expanded square grid layers has been anticipated to occur on the crystal self-assembly. Interpenetration, which is known[2] to mitigate against the existence of nets with very large cavities, could thus enter the stage. Resolvability of the binaphthyl tecton **2** provided us the opportunity to observe homochiral as well as heterochiral interpenetration of the enantiomerically uniform 2D square grid layers.

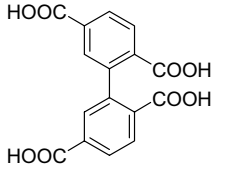

1

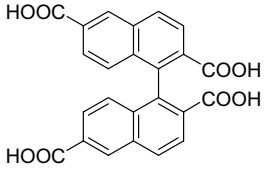

2

2. Results and discussion

2.1. Synthesis

Bromination of 6-methylnaphthalene-2-carboxylic acid **3** gave the 5-bromo-derivative **4**, which on oxidation

* Corresponding author. Tel.: +420 220 183 382; fax: +420 220 183 560; e-mail: petrholy@uochb.cas.cz

0957-4166/$ - see front matter © 2005 Elsevier Ltd. All rights reserved.
doi:10.1016/j.tetasy.2005.04.018

yielded 1-bromonaphthalene-2,6-dicarboxylic acid **5**. Esterification followed by C–C coupling in the presence of activated copper bronze afforded tetraester **7** and after subsequent hydrolysis the target tetraacid (*RS*)-**2** (Scheme 1). While attempts to resolve the racemic tetraacid **2** with chiral amines failed, we succeeded in the separation of the diastereoisomeric tetramenthyl esters **9a** and **9b** arising from the esterification of racemic acid **2** with (−)-menthol. Preparative TLC of the diastereoisomeric mixture, followed by hydrolysis, afforded the corresponding enantiomers of the tetraacid **2** (Scheme 2), with their absolute configurations assigned on the basis of X-ray crystallographic analysis of one of the diastereoisomeric tetramenthyl esters.

2.2. X-ray crystallographic analysis

As the crystallographic X-ray analysis of the racemic tetraacid (*RS*)-**2** showed, both antipode molecules (*R*)-**2** and (*S*)-**2** are built from one (identical) half of the molecular structure via symmetry operations with all bond angles and distances being unexceptional. The naphthalene core is slightly bent with the dihedral angle between the least square planes of the condensed benzene rings being 0.73(12)°. The adjacent carboxyl carbons (C11 and C12) lay nearly in the naphthalene least square plane, and also the planes of the carboxyl groupings do not diverge substantially, the pertinent dihedral angles being 13.52(39)° and 8.42(44)°, respectively. In accordance with expectations, the dihedral angle between the coupled naphthalene rings [80.90(3)°] approaches rectangularity (Fig. 1a). A marked bending occurs along the biaryl junction, the observed perpendicular distances from the least square plane of the C1–C2–C3–C4–C10–C9 ring for C1′ and C4′ atoms of the attached aryl being 0.119(3) and 0.495(5) Å, respectively. The molecular structure of (*R*)-**2** in the homochiral crystal is very similar (Fig. 1b).

2.2.1. Self-assembly of hydrogen-bonded square grid layers and their stacking. In the crystal of the racemic as well as the homochiral tetraacid **2**, individual tectons are organized via intermolecular hydrogen bonds. All carboxyl groups are involved in this organization, each participating simultaneously as a donor and acceptor in the formation of one double hydrogen bond. The binaphthyl tectons are thus chained, in one direction, via the carboxyl groups placed alternately at the 2- and 6-positions, whereas, the corresponding carboxyls, which are placed in the 2′- and 6′-positions create another chain proceeding in a nearly perpendicular direction. A combination of the two divergent chains leads to the formation of infinite 'square' grid layers set up from hydrogen-bonded cyclotetrameric compartments (Fig. 2a and b).

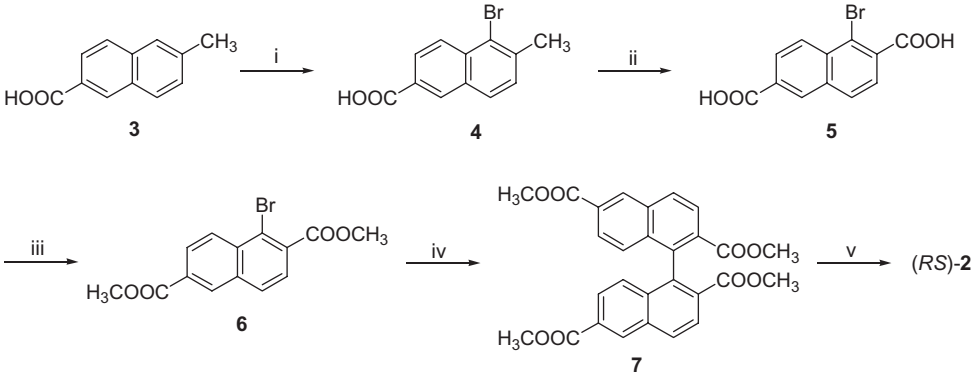

Scheme 1. Reagents and conditions: (i) Br_2, CH_3COOH, 80%; (ii) O_2, $Co(CH_3COO)_2$, CH_3COOH, $CH_3COC_2H_5$, 70%; (iii) CH_3OH, H_2SO_4, 78%; (iv) Cu, DMF, 76%; (v) NaOH, $EtOH/H_2O$, then 1 M HCl, 96%.

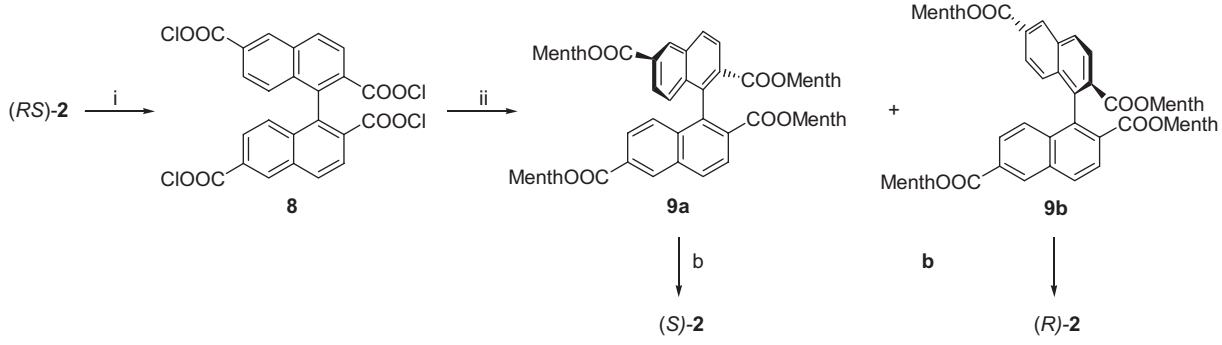

Scheme 2. Reagents and conditions: (i) $SOCl_2$, then (−)-menthol, pyridine, DMAP, preparative TLC; (ii) KOH, CH_3OH, then 1 M HCl; overall yields from (*RS*)-**2**: (*S*)-**2** 20% and (*R*)-**2** 27%.

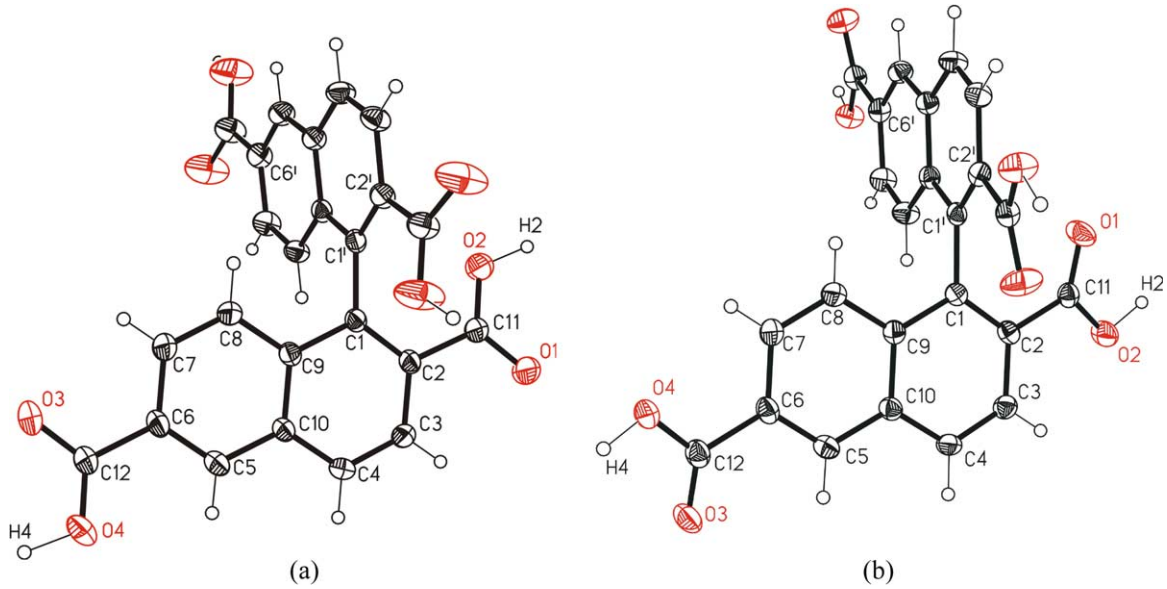

Figure 1. Molecular structure of (*R*)-**2** in the crystals of the racemic (a) and the homochiral tecton (b). Ellipsoids for 50% probability.

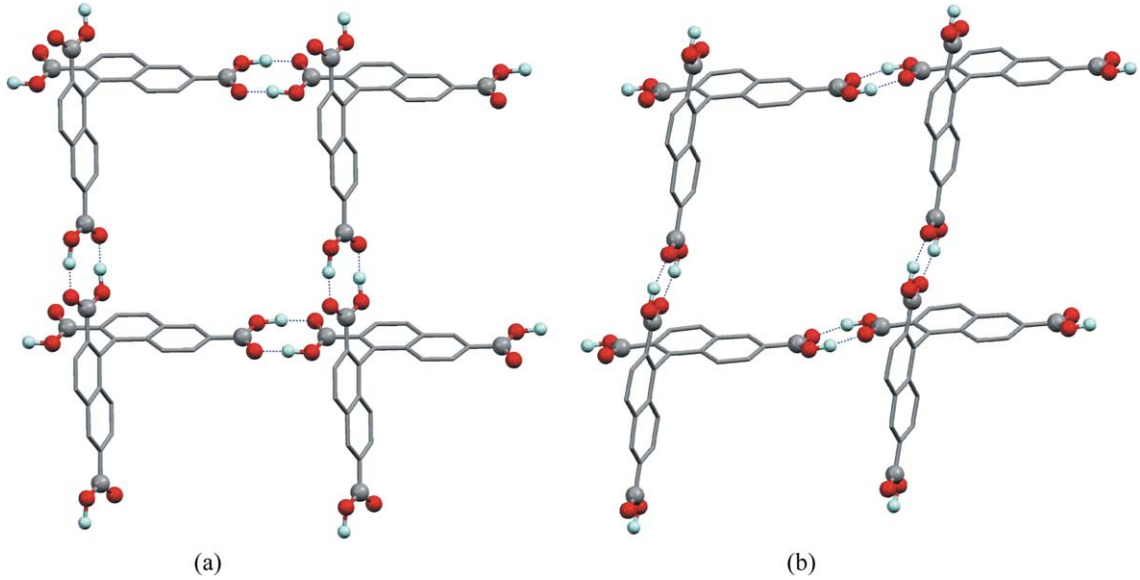

Figure 2. Self-assembly of hydrogen-bonded square grid layers set up from cyclotetrameric compartments. Cyclotetrameric compartments relate to self-assembly from (*R*)-**2** tectons in the racemic (a) and homochiral (b) crystal; simplified drawing of aromatic rings (carboxyls in ball and stick mode).

A unique stereochemical feature of this self-organization process is that its algorithm requires homochiral tectons. This leads to homochiral 'square' grid layers, which are organized into homochiral stacks of the layers. Remarkably, such a sequence of self-assembling homochiral steps takes place in the homochiral as well as in the racemic crystal of tecton **2**, vide infra.

2.2.2. 3D polycatenation of the stacked 2D layers. In the crystal of (*RS*)-**2**, tectons of opposite chirality are in this way segregated into antipodal stacks of staggered homochiral square grid layers. Both the antipodal stacks are arranged perpendicular with respect to the other and integrated by a mutual interpenetration. Nodes from one network are placed in complementary square cavities of the other (antipodal) network, and vice versa, so that the catenation proceeds in a diagonal/diagonal[4] fashion (Fig. 3a). In contrast the crystal of (*R*)-**2**, three independent stacks of the grid layers, inclined each in the respect to the other two at 120° angle, are mutually interpenetrated. The catenation proceeds in a parallel/parallel/parallel[4] fashion (Fig. 3b), at variance with the racemic crystal.

Steric overcrowding, which might arise as a consequence of the threefold catenation in the homochiral crystal, is diminished by expanding the size of the cyclotetrameric compartments via stretching the intermolecular hydrogen

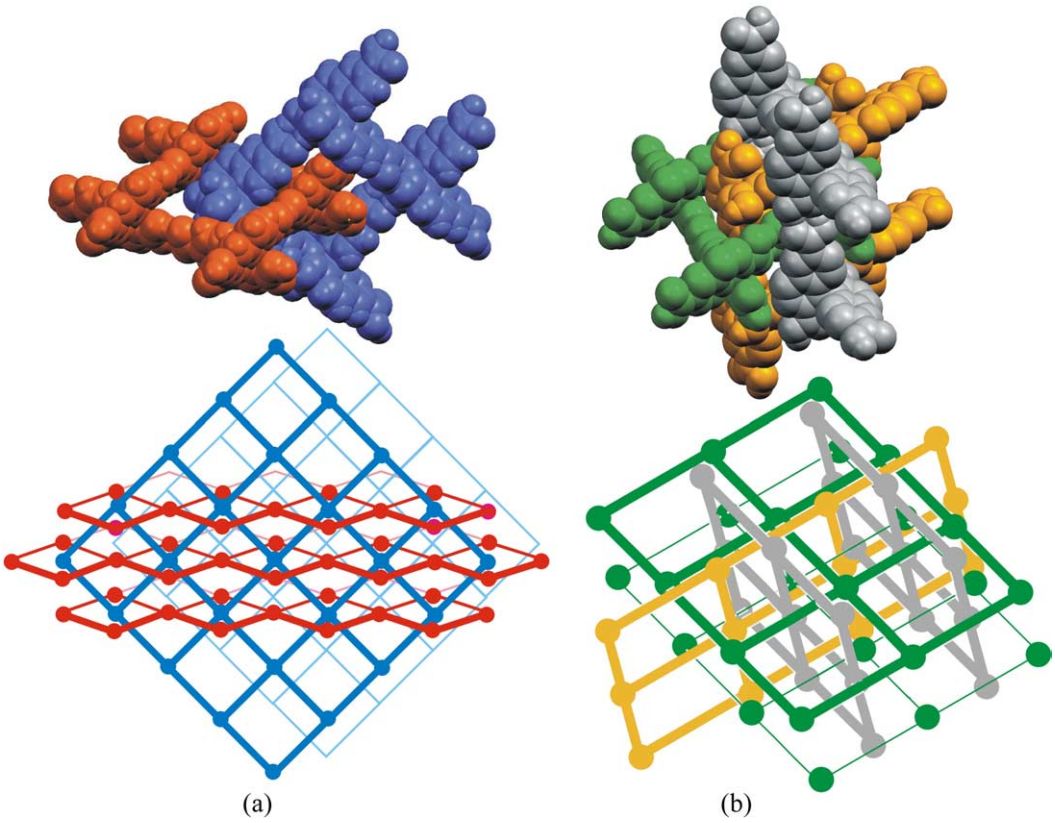

Figure 3. (a) Diagonal/diagonal catenation of the antipodal square grids in the crystal of racemic tetraacid (*RS*)-**2** versus (b) parallel/parallel/parallel catenation in the crystal of (*R*)-**2**.

bonds. The carboxyl–carboxyl hydrogen bonds are much longer (1.66 and 1.67 Å) than those found in the racemic form (1.51 and 1.52 Å) (Table 1). The threefold catenation induces a higher density (1.445 g cm^{-3}), markedly exceeding the corresponding value found for the racemic crystal (1.292 g cm^{-3}).

In accordance, the PLATON program[5] indicates a more effective utilization of the interior of the squares in the homochiral crystal, the residual empty space being substantially smaller (7.5%) than in the racemic form (16%).

2.2.3. Overview of known interpenetrating chiral nets. Batten and Robson in their seminal study[2a] summarized and classified a wide array of 2D and 3D *interpenetrating* nets discovered by X-ray crystallographic analysis. Some of the known interpenetrating nets are chiral, belonging mostly among three- or four-connected 3D nets. In contrast to the prevalent 3D chiral nets, only one example has been traced in literature concerning interpenetration of chiral 2D nets.[6] This, moreover, can be regarded to be a 'bastard case', involving a mutual interpenetration of one chiral and one achiral net.

3. Conclusions

Herein we have investigated the interpenetration of chiral 2D nets self-assembled from chiral tectons, representing an intriguing but hitherto unexplored stereochemical problem. The axially chiral tetraacid **2** turned out to be an excellent tecton for such an investigation, allowing us to follow the stereochemical aspects of the overall process in three conceptually distinct steps, (i) formation of infinite 2D grid nets set up from hydrogen-bonded cyclotetramers, (ii) formation of stacks of the 2D grid nets, and (iii) interpenetration of the stacks of layers resulting in 3D polycatenated crystal architecture.

Table 1. Parameters of hydrogen bonds in the investigated crystals

Compound	Specification	Distances (Å)			Bond angle (°)
	O–H···O	O–H	H···O	O···O	O–H···O
(*RS*)-**2**	O2–H2···O3	1.06(2)	1.51(3)	2.569(2)	177(2)
	O4–H4···O1	1.13(3)	1.52(3)	2.632(2)	163(2)
(*R*)-**2**	O2–H2···O3	1.03(2)	1.67(3)	2.6960(14)	167(2)
	O4–H4···O1	0.96(2)	1.66(2)	2.6141(14)	171(2)

Enantioselectivity of the individual steps has been investigated in a parallel study of the enantiomerically uniform and racemic tecton **2**. In the self-assembly of the enantiomerically uniform tecton, all the participating processes are by definition homochiral. The racemic tecton follows the homochiral self-assembling algorithm only in steps (i) and (ii) giving rise to separate, antipodal, stacks of homochiral 2D layers. In the final step (iii), the antipodal stacks mutually interpenetrate, giving rise to racemic 3D polycatenated architecture within a single crystal. Aside from this unique enantiodifferentiation, several other remarkable features distinguishing the homochiral and heterochiral polycatenation have been at the same time established.

4. Experimental

4.1. General

Melting points were determined on a Kofler apparatus and are uncorrected. NMR spectra were measured on a Bruker AVANCE 400 (^{1}H at 400 MHz) and a Varian UNITY 500 spectrometers (^{1}H at 500 MHz; ^{13}C at 125.7 MHz) in $CDCl_3$ or in DMSO. Chemical shifts (δ in parts per million) are referenced either to TMS (^{1}H in $CDCl_3$) or residual solvent signal (δ_H(DMSO) = 2.50; δ_C($CDCl_3$) = 77.0; δ_C(DMSO) = 39.7). Coupling constants J are given in hertz. Mass spectra were recorded on a ZAB-EQ (VG-Analytical) instrument (EI-70 eV, FAB-Xe, 8 kV). Thioglycerol-glycerol and 2-hydroxyethyl disulfide matrices were used for the FAB technique.

4.2. Synthesis

4.2.1. 6-Methylnaphthalene-2-carboxylic acid 3. Prepared from 2-acetyl-6-methylnaphthalene by hypobromite oxidation[7,8] in 85.3% yield; mp 234 °C, Lit.[7] 229 °C, Lit.[8] 230 °C. Anal. Calcd for $C_{12}H_{10}O_2$ (186.21): C, 77.40; H, 5.41. Found: C, 77.32; H, 5.25. MS (EI): *m/z* 186 (M^+, 100), 169 (22), 141 (40), 115 (12). ^{1}H NMR (400 MHz, DMSO): δ 2.5 (s, 3H, CH_3); 7.45 (dd, 1H, H-3, J(3,4) = 8.4, J(3,1) = 1.6); 7.76 (dd, 1H, H-1, J(1,3) = 1.6, J(1,5) = 0.6); 7.89 (d, 1H, H-8, J(8,7) = 8.4); 7.94 (dd, 1H, H-7, J(7,8) = 8.4, J(7,5) = 1.7); 8.00 (d, 1H, H-4, J(4,3) = 8.4); 8.55 (dd, 1H, H-5, J(5,7) = 1.7, J(5,1) = 0.6); 12.95 (br s, 1H, COOH).

4.2.2. 5-Bromo-6-methylnaphthalene-2-carboxylic acid 4. Bromine (5.0 mL, 98 mmol) in acetic acid (70 mL) was added dropwise at 50 °C to the stirred solution of acid **3** (14.93 g, 80.2 mmol) in acetic acid (930 mL). The reaction mixture was kept at 50 °C for 10 h and then concentrated in vacuo to 300 mL. The crystalline deposit was sucked off and washed with a small amount of acetic acid. Yield after crystallization from ethanol 17.10 g (80%), mp 274–277 °C. Anal. Calcd for $C_{12}H_9BrO_2$ (265.10) C, 54.37; H, 3.42; Br, 30.14. Found: C, 54.17; H, 3.32; Br, 30.19. EI MS: *m/z* 266 (M^+, 100), 247/249 (12), 219/221 (10), 185 (60), 139 (62), 115 (17), 69 (14), 63 (15).^{1}H NMR (400 MHz, DMSO): δ 2.60 (s, 3H, CH_3); 7.60 (d, 1H, H-7, J(7,8) = 8.4); 8.08 (d, 1H, H-8, J(8,7) = 8.4); 8.10 (dd, 1H, H-3, J(3,4) = 8.9, J(3,1) = 1.7); 8.25 (d, 1H, H-4, J(4,3) = 8.9); 8.61 (d, 1H, H-1, J(1,3) = 1.7); 13.20 (br s, 1H, COOH).

4.2.3. 1-Bromonaphthalene-2,6-dicarboxylic acid 5. Into a stirred solution of bromo acid **4** (7.00 g, 26.4 mmol) and cobalt(II) acetate tetrahydrate (1.75 g, 7.02 mmol) in acetic acid (500 mL) and 2-butanone (25 mL), a slow stream of oxygen was introduced at 105 °C for 8 h. Additional portions of 2-butanone (10 mL) were added in 2 h intervals. After cooling, the volume was reduced to 200 mL in vacuo. The crude diacid was filtered off, dried, and crystallized from hot toluene. Yield 5.45 g (70%), mp 350–355 °C. Anal. Calcd for $C_{12}H_7BrO_4$ (295.09): C, 48.84; H, 2.39; Br, 27.08. Found: C, 48.95; H, 2.35; Br, 26.75. EI MS: *m/z* 294/296 (M^+, 100), 277/279 (52), 249/251 (17), 216 (70), 199 (42), 171 (29), 125 (19), 115 (11), 98 (13), 83 (12), 73 (13), 71 (13), 57 (19), 55 (14), 43 (15), 28 (12). ^{1}H NMR (400 MHz, DMSO): δ 7.74 (d, 1H, H-3, J(3,4) = 8.4); 8.19 (dd, 1H, H-7, J(7,8) = 8.9, J(7,5) = 1.6); 8.25 (d, 1H, H-4, J(4,3) = 8.4); 8.40 (d, 1H, H-8, J(8,7) = 8.9); 8.75 (d, 1H, H-5, J(5,7) = 1.6); 13.55 (br s, 2H, COOH).

4.2.4. Dimethyl 1-bromonaphthalene-2,6-dicarboxylate 6. A mixture of bromodicarboxylic acid **5** (16.27 g, 55.14 mmol), absolute methanol (1000 mL), and concd sulfuric acid (30 mL) was heated at reflux for 48 h. After concentration to 300 mL, the precipitated diester was filtered off and dissolved in boiling methanol (700 mL). The solution was decolorized with activated carbon, filtered, and left in a refrigerator. The crystallized diester was collected on filter and dried. Yield 13.87 g (77.9%), mp 126–127 °C. Anal. Calcd for $C_{14}H_{11}BrO_4$ (323.14): C, 52.04; H, 3.43; Br, 24.73. Found: C, 51.94; H, 3.27; Br, 24.75. EI MS: *m/z* 322/324 (M^+, 96), 291/293 (100), 263/265 (11), 248/250 (12), 232/234 (8), 204/206 (6), 153 (18), 125 (36), 83 (10), 69 (19), 57 (18), 43 (14), 28 (30). ^{1}H NMR (500 MHz, $CDCl_3$): δ 4.00 (s, 3H, OCH_3); 4.02 (s, 3 H, OCH_3); 7.71 (d, 1H, H-3, J(3,4) = 8.5); 7.94 (dt, 1H, H-4, J(4,3) = 8.5, J(4,5) = 0.7, J(4,8) = 0.8); 8.19 (dd, 1H, H-7, J(7,8) = 8.9, J(7,5) = 1.7); 8.48 (dt, 1H, H-8, J(8,7) = 8.9, J(8,4) = 0.8, J(8,5) = 0.7); 8.58 (dt, 1H, H-5, J(5,7) = 1.7, J(5,4) = 0.7, J(5,8) = 0.7). ^{13}C NMR (125.7 MHz, $CDCl_3$): 52.49 and 52.83 (2 × OCH_3); 122.22 (C-10); 126.45 (C-3); 127.33 (C-7); 128.95 (C-8); 129.08 (C-4); 129.46 (C-6); 130.92 (C-5); 133.42 (C-2); 134.24 (C-1); 134.32 (C-9); 166.38 and 167.51 (2 × C═O).

4.2.5. Tetramethyl 1,1′-binaphthalene-2,2′,6,6′-tetracarboxylate 7. A mixture of bromodimethyl ester **6** (5.03 g, 15.58 mmol) and activated[9] copper bronze (5.00 g, 78.7 mmol) in DMF (15 mL) was heated at 150 °C for 2.5 h. The hot mixture was filtered and insoluble portions extracted with hot toluene (3 × 150 mL). The combined filtrates were successively washed with 2 M HCl (100 mL), saturated aqueous solution of $NaHCO_3$ (100 mL), and water (2 × 100 mL). After drying over $MgSO_4$ the solvents were evaporated and the residue (3.80 g) was extracted with boiling toluene

(2 × 100 mL). Petroleum ether (150 mL) was gradually added to the combined extracts. The crystalline precipitate was filtered off and dried. Yield 2.88 g (76.1%), mp 220–224 °C. Anal. Calcd for $C_{28}H_{22}O_8$ (486.47): C, 69.13; H, 4.56. Found: C, 68.95; H, 4.44. MS (EI): *m/z* 486 (M^+, 100), 455 (21), 427 (14), 396 (8), 278 (7), 212 (12), 125 (7), 91 (78), 62 (12), 43 (17), 28 (36). ^{1}H NMR (500 MHz, $CDCl_3$): δ 3.51 (s, 3H, OCH_3); 3.96 (s, 3H, OCH_3); 7.09 (dt, 1 H, H-8, J(8,7) = 8.9, J(8,4) = 0.8, J(8,5) = 0.8); 7.81 (dd, 1H, H-7, J(7,8) = 8.9, J(7,5) = 1.7); 8.15 (dd, 1H, H-4, J(4,3) = 8.6, J(4,8) = 0.8); 8.24 (d, 1H, H-3, J(3,4) = 8.6); 8.71 (dd, 1H, H-5, J(5,7) = 1.7, J(5,8) = 0.8). ^{13}C NMR (125.7 MHz, $CDCl_3$): 52.10 and 52.38 (2 × OCH_3); 139.44 (C-10); 126.73 (C-3); 126.19 (C-7); 127.33 (C-8); 129.44 (C-4); 129.13 (C-6); 130.93 (C-5); 129.21 (C-2); 134.02 (C-1); 134.86 (C-9); 166.64 and 166.86 (2 × C=O).

4.2.6. Racemic 1,1′-binaphthalene-2,2′,6,6′-tetracarboxylic acid (*RS*)-2. Tetramethyl ester **7** (7.03 g, 14.45 mmol) was treated with sodium hydroxide (4.26 g, 107 mmol) dissolved in water (200 mL) and ethanol (100 mL) under reflux for 10 h and the resulting mixture concentrated to 150 mL in vacuo. After extraction with ether (2 × 30 mL), the aqueous phase was acidified with 2 M HCl to pH 1. The precipitated tetra acid was filtered off, washed with water, and crystallized from aqueous acetone. Crystals were separated and dried in vacuo (20 Pa, 6 h, rt), yield 6.38 g (96%), mp >360 °C. Anal. Calcd for $C_{24}H_{14}O_8 \cdot 1/2\ C_3H_6O$ (459.40): C, 66.67; H, 3.73. Found: C, 66.62; H, 3.83. MS (EI): *m/z* 430 (M^+, 28), 386 (6), 368 (5), 340 (3), 323 (4), 296 (5), 252 (10), 216 (100), 199 (53), 171 (40), 126 (20), 115 (27), 97 (14), 91 (16), 77 (27), 55 (38), 41 (44), 28 (53). ^{1}H NMR (400 MHz, DMSO): δ 6.98 (d, 1H, H-8, J(8,7) = 8.9); 7.76 (dd, 1H, H-7, J(7,8) = 8.9, J(7,5) = 1.8); 8.14 (d, 1H, H-4, J(4,3) = 8.7); 8.32 (d, 1H, H-3, J(3,4) = 8.7); 8.72 (d, 1H, H-5, J(5,7) = 1.8); 12.95 (br s, 1H, COOH).

Crystals for X-ray analysis were grown from aqueous methanol by a slow evaporation of the solvent.

4.2.7. Racemic 1,1′-binaphthalene-2,2′,6,6′-tetra(carbonylchloride) 8. A mixture of tetraacid (*RS*)-**2** (2.00 g, 4.41 mmol), thionyl chloride (80 mL), and a drop of DMF was heated at reflux for 5 h. Excess thionyl chloride was removed in vacuo, and the solid residue (2.23 g) taken up in boiling toluene (2 × 50 mL) and crystallized on addition of petroleum ether to the toluene solution. Yield 1.99 g (90%), mp 213–216 °C. Anal. Calcd for $C_{24}H_{10}ClO_4$ (504.15): C, 57.18; H, 2.00; Cl, 28.13. Found: C, 57.15; H, 1.88; Cl, 28.14. ^{1}H NMR (400 MHz, $CDCl_3$): δ 7.10 (d, 1H, H-8, J(8,7) = 9.0); 7.92 (dd, 1H, H-7, J(7,8) = 9.0, J(7,5) = 1.9); 8.37 (d, 1H, H-4, J(4,3) = 8.8); 8.50 (d, 1H, H-3, J(3,4) = 8.8); 8.90 (d, 1H, H-5, J(5,7) = 1.9).

4.2.8. Tetra-[(1*R*,2*S*,5*R*)-menthyl] (*S*)-1,1′-binaphthalene-2,2′,6,6′-tetracarboxylate 9a and tetra-[(1*R*,2*S*,5*R*)-menthyl] (*R*)-1,1′-binaphthalene-2,2′,6,6′-tetracarboxylate 9b. A solution of freshly prepared racemic tetra(carbonylchloride) **8** (250 mg; 0.496 mmol), (1*R*,2*S*,5*R*)-(−)-menthol (359 mg; 2.3 mmol), and 4-dimethylaminopyridine (20 mg) in pyridine (2 mL) was heated at 110 °C for 6 h. After cooling, the mixture was partitioned between water and ether, the ethereal layer washed with dilute HCl, water, $NaHCO_3$ solution, and stripped of the solvent. The resulting solid foam was disintegrated, treated with a small amount of methanol to remove the unreacted menthol, and the insoluble product was collected on filter; weight 491 mg. Separation by preparative TLC on silica gel (Merck, 20 × 20 cm, thickness 2 mm, ether–petroleum ether 1:10, five 100 mg batches) followed by two crystallizations of each fraction from 2-propanol afforded pure diastereoisomers **9a** and **9b**.

Compound **9a** (lower R_f value): yield 105 mg (22%), mp 198–200 °C, $[\alpha]_D^{20} = -66.6$ (c 0.2, $CHCl_3$). Anal.

Table 2. ^{1}H and ^{13}C NMR chemical shifts in diastereoisomers **9a** and **9b**

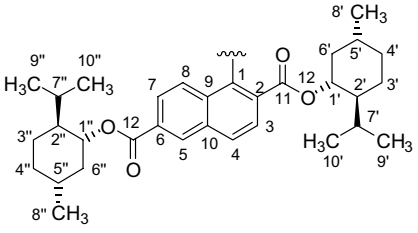

Position	Proton chemical shifts		Carbon-13 chemical shifts	
	9a	**9b**	**9a**	**9b**
1	—	—	134.23	133.96
2	—	—	129.90	129.96
3	8.298	8.297	127.22	127.31
4	8.162	8.163	129.06	129.11
5	8.683	8.685	130.39	130.63
6	—	—	129.82	129.72
7	7.848	7.804	126.28	126.03
8	7.225	7.083	127.42	127.80
9	—	—	135.26	135.27
10	—	—	139.46	139.20
11	—	—	166.00	166.21
12	—	—	165.69	165.65
1′	4.45	4.52	74.58	74.83
2′	0.47	0.22	46.36	46.14
3′	0.75	0.75	22.46	22.33
4′	1.57; 1.73	0.58; 1.51	33.89	33.92
5′	1.15	1.27	30.80	31.43
6′	−0.53; 1.27	0.31; 1.64	39.39	40.08
7′	1.40	0.66	25.75	25.04
8′	0.57 (3H)	0.78 (3H)	21.71	21.86
9′	0.70 (3H)	0.30 (3H)	20.83	20.61
10′	0.48 (3H)	0.39 (3H)	15.47	15.21
1″	4.97	4.97	75.18	75.18
2″	1.57	1.56	47.28	47.27
3″	1.15; 1.73	1.15; 1.74	23.64	23.58
4″	0.94; 1.73	0.94; 1.74	34.28	34.27
5″	1.56	1.56	31.44	31.15
6″	1.12; 2.12	1.10; 2.12	40.92	40.88
7″	1.92	1.94	26.57	26.51
8″	0.93 (3H)	0.925 (3H)	22.02	22.01
9″	0.89 (3H)	0.78 (3H)	20.70	21.86
10″	0.775 (3H)	0.78 (3H)	16.51	16.44

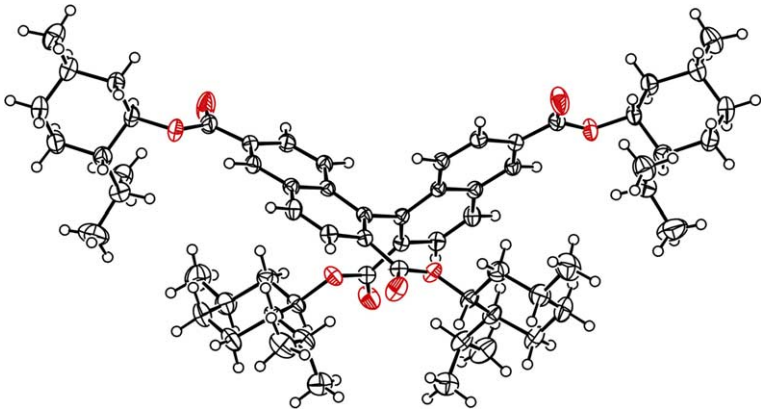

Figure 4. Molecular structure of the diastereoisomer **9a**.

Calcd for $C_{64}H_{86}O_8$ (983.36): C, 78.17; H, 8.81. Found: C, 78.00; H, 9.07. MS (FAB): *m*/*z* 983 (18), 984 (15), 827 (9), 689 (100), 640 (10), 583 (10), 551 (95), 527 (15), 507 (26).

Compound **9b** (higher R_f value): yield 146 mg (30%), mp 157–159 °C, $[\alpha]_D^{20} = -109.5$ (*c* 0.2, $CHCl_3$). Anal. Calcd for $C_{64}H_{86}O_8$ [983.36]: C, 78.17; H, 8.81. Found: C, 78.17; H, 9.03. MS (FAB): *m*/*z* 983 (7), 909 (5), 689 (97), 661 (10), 638 (6), 581 (10), 567 (17), 552 (22), 551 (100), 535 (10), 525 (22), 507 (25).

The unambiguous assignment of the signals in ^1H and ^{13}C NMR spectra of both diastereoisomers was achieved by a combination of 1D-^1H NMR, 2D-^1H, ^1H-COSY, ^{13}C-APT, 2D-^1H, ^{13}C-HSQC, and 2D-^1H, ^{13}C-HMBC spectra. The NMR data of diastereoisomers **9a** and **9b** together with the numbering of carbon atoms in one half of the molecule are given in Table 2. A single crystal of diastereoisomer **9a** for X-ray measurement was obtained by slow cooling of ethanolic solution. The molecular structure of diastereoisomer **9a** is shown in Figure 4.

4.2.9. (+)-(*S*)-1,1′-Binaphthalene-2,2′,6,6′-tetracarboxylic acid (*S*)-2. Tetraester **9a** (47 mg; 0.05 mmol) was heated with a methanolic solution of KOH (500 mg in 3 mL) in an autoclave at 110 °C for 6 h. Milder

Table 3. Crystallographic data

Compound	(*RS*)-**2**	(*R*)-**2**	**9a**
Formula	$C_{24}H_{14}O_8$	$C_{24}H_{14}O_8$	$C_{64}H_{86}O_8$
M_r	430.35	430.35	983.33
Crystal system	Tetragonal	Trigonal	Tetragonal
Space group	*I*-4	*R*32	$P4_32_12$
T (K)	150(2)	150(2)	150(2)
a (Å)	11.3510(2)	14.3430(2)	14.9340(2)
b (Å)	11.3510(2)	14.3430(2)	14.9340(2)
c (Å)	17.1710(4)	24.9860(3)	26.1680(3)
α (°)	90.00	90.00	90.00
β (°)	90.00	90.00	90.00
γ (°)	90.00	120.00	90.00
Z	4	9	4
V ((Å)^3)	2212.40(8)	4451.5(1)	5836.1(1)
D_c (g cm^{-3})	1.292	1.445	1.119
Crystal dimensions (mm)	0.4 × 0.25 × 0.25	0.3 × 0.25 × 0.15	0.6 × 0.35 × 0.35
Appearance	Colorless prism	Colorless prism	Colorless prism
μ (mm^{-1})	0.098	0.110	0.072
θ Range	2.37–27.5	1.83–27.5	1.0–27.5
h Range	−14, 14	−18, 18	−19, 19
k Range	−10, 10	−15, 15	−13, 13
l Range	−22, 22	−32, 32	−32, 32
Reflections measured	19,003	38,180	59,701
Independent (R_{int})	2529 (0.032)	2294 (0.035)	6679 (0.038)
Observed [$I > 2\sigma(I)$]	2321	2171	5871
Parameters refined	145	154	331
S	1.073	1.025	1.026
R	0.052	0.031	0.036
wR	0.155	0.081	0.089
$\Delta\rho_{max}$; $\Delta\rho_{min}$ (e Å^{-3})	0.609; −0.228	0.217; −0.166	0.235; −0.197

saponification conditions (boiling with methanolic KOH) led exclusively to partial hydrolysis of the 6,6′-ester groups affording the 2,2′-dimenthyl ester. The mixture was partitioned between ether and water, and the aqueous phase was taken down in vacuo. The residue was dissolved in minimum volume of water, acidified with concd HCl, and extracted several times with ether. The ethereal phase afforded 20 mg of tetraacid (+)-(*S*)-**2**, not melting up to 360 °C, $[\alpha]_D^{20} = +59.0$ (*c* 0.15, methanol); ^{1}H NMR spectrum (400 MHz, DMSO) was identical with that of the racemate.

4.2.10. (−)-(*R*)-1,1′-Binaphthalene-2,2′,6,6′-tetracarboxylic acid (*R*)-2. Using the same procedure, 50 mg of tetraester **9b** afforded 21.5 mg of acid (−)-(*R*)-**2**, not melting up to 360 °C, $[\alpha]_D^{20} = -61.5$ (*c* 0.17, methanol); ^{1}H NMR spectrum identical with that of the racemate. Anal. Calcd for $C_{24}H_{14}O_8 \cdot H_2O$: C, 64.29; H, 3.60. Found: C, 64.74; H, 3.70.

Crystals for X-ray analysis were grown from aqueous acetone by free evaporation of the solvent.

4.3. X-ray diffraction analysis

X-ray data were collected on a Nonius KappaCCD diffractometer, Mo K_α radiation ($\lambda = 0.71073$ Å, graphite monochromator) at 150(2) K, ω-scans. Data were corrected on LP factor, absorption was neglected. The structures were solved by direct methods (SIR[10]) and refined by least squares methods based on F^2 with all measured reflections, all non-hydrogen atoms are refined anisotropically (SHELXL97[11]). Hydrogen atoms of naphthalene moiety were calculated into idealized positions and refined as riding on their pivot atom with assigned temperature factors $H_{iso}(H) = 1.2\ U_{eq}$(pivot atom) or $H_{iso}(H) = 1.5\ U_{eq}$(pivot atom) for methyl moiety.

Crystal data, measurement, and refinement details are summarized in Table 3.

All crystallographic data for the investigated structures have been deposited with the Cambridge Crystallographic Data Centre as supplementary publication numbers: (*RS*)-**2** CCDC 261003, (*R*)-**2** CCDC 261004 and **9a** CCDC 261005. Copies of the data can be obtained, free of charge, on application to CCDC, 12 Union Road, Cambridge, CB2 1EZ, UK (fax: +44(0) 1223 336033 or e-mail: deposit@ccdc.cam.ac.uk).

Acknowledgements

This work is part of research project Z4 055 905. The financial support provided by the Grant Agency of the Czech Republic to the authors (grant No. 203/03/0087) and to the Center of Molecular and Crystal Structure (grant No. 203/99/M037) is gratefully acknowledged.

References

1. (a) *Templated Organic Synthesis*; Diederich, F., Stang, P. J., Eds.; Wiley-VCH: Weinheim, 2000; (b) *Molecular Catenanes, Rotaxanes and Knots*; Sauvage, J.-P., Dietrich-Buchecker, C., Eds.; Wiley-VCH: Weinheim, 1999; (c) Fujita, M. *Acc. Chem. Res.* **1999**, *32*, 53–61; (d) Vögtle, F.; Dunwald, T.; Schmidt, T. *Acc. Chem. Res.* **1996**, *29*, 451–460; (e) Kidd, T. J.; Leigh, D. A.; Wilson, A. J. *J. Am. Chem. Soc.* **1999**, *121*, 1599–1600; (f) Hubin, T. J.; Busch, D. H. *Coord. Chem. Rev.* **2000**, *200–202*, 5–52; (g) Rahm, L.; Hamilton, D. G.; Sanders, J. K. M. *Synlett* **2002**, 1743–1761; (h) Amabilino, D. B.; Stoddart, J. F. *Chem. Rev.* **1995**, *95*, 2725–2828.
2. (a) Batten, S. R.; Robson, R. *Angew. Chem., Int. Ed.* **1998**, *37*, 1460–1494; (b) Moulton, B.; Zaworotko, M. J. *Chem. Rev.* **2001**, *101*, 1628–1658.
3. (a) Holý, P.; Závada, J.; Císařová, I.; Podlaha, J. *Angew. Chem., Int. Ed.* **1999**, *38*, 381–383; (b) Tichý, M.; Kraus, T.; Závada, J.; Císařová, I.; Podlaha, J. *Tetrahedron: Asymmetry* **1999**, *10*, 3277–3280; (c) Holý, P.; Závada, J.; Císařová, I.; Podlaha, J. *Tetrahedron: Asymmetry* **2001**, *12*, 3035–3045; (d) Kraus, T.; Císařová, I.; Buděšínský, M.; Závada, J. *Angew. Chem., Int. Ed.* **2002**, *41*, 1715–1717; (e) Holý, P.; Sehnal, P.; Tichý, M.; Závada, J.; Císařová, I. *Tetrahedron: Asymmetry* **2003**, *13*, 245–253.
4. Biradha, K.; Mondal, A.; Moulton, B.; Zaworotko, M. J. *J. Chem. Soc. Dalton Trans.* **2000**, 3837–3844.
5. Spek, L. PLATON, *A Multipurpose Crystallographic Tool*; Utrecht University: Utrecht (The Netherlands), 2004.
6. Biradha, K.; Domasevitch, K. V.; Moulton, B.; Sewald, C.; Zaworotko, M. J. *Chem. Comm.* **1999**, 1327–1328.
7. Friese, V.; Boos, A.; Bauch, H.-J.; Leistner, E. *Phytochemistry* **1993**, *32*, 616–622.
8. Kon, R.; Weller, W. T. *J. Chem. Soc.* **1939**, 792–794.
9. *Vogel's Textbook of Practical Organic Chemistry*; Furniss, B. S., Hannaford, A. J., Tatchell, A. R., Eds., 5th ed.; John Wiley & Sons: New York, 1989, p 426.
10. Altomare, A.; Cascarano, G.; Giacovazzo, C.; Guagliardi, A.; Burla, M. C.; Polidori, G.; Camalli, M. *J. Appl. Crystallogr.* **1994**, *27*, 435.
11. Sheldrick, G. M. SHELXL-97. *A Program for Crystal Structure Refinement*; University of Göttingen, Germany, 1997.